27. R. K. Dixon *et al.*, *Science* **263**, 185 (1994).
28. I. A. Janssens *et al.*, *Science* **300**, 1538 (2003).
29. J. Lloyd, G. D. Farquhar, *Funct. Ecol.* **10**, 4 (1996).
30. S. R. Saleska *et al.*, *Science* **302**, 1554 (2003).
31. K. W. Holmes *et al.*, *Global Biogeochem. Cycles* **20**, GB3004 (2006).
32. A. D. McGuire *et al.*, *Global Biogeochem. Cycles* **15**, 183 (2001).
33. D. F. Baker *et al.*, *Global Biogeochem. Cycles* **20**, GB1002 (2006).
34. We thank the following T3L2 modelers for sharing their model output with us: R. M. Law, P. J. Rayner, D. Baker, Y.-H. Chen, I. Y. Fung, S. Houweling, J. John, T. Maki, S. Maksyutov, P. Peylin, M. Prather, B. C. Pak, and S. Taguchi. We thank A. Jacobson for helpful discussions. This work was supported by funding from the NSF, which sponsors the National Center for Atmospheric Research. The Transcom 3 experiment was made possible through support from the NSF (OCE-9900310), the National Oceanic and Atmospheric Administration (NA67RJ0152, Amend 30), and the International Geosphere Biosphere Program/Global Analysis, Interpretation, and Modeling Project. The Zotino measurements are supported by the European Union through the TCOS-Siberia contract (EVK2-CT-2001-00131) within the Fifth Framework Program. The Bass Strait/Cape Grim aircraft sampling program was supported by the Australian Bureau of Meteorology (1992–98), and the CSIRO Office of Space Science and Applications (1999–2000).

Supporting Online Material

www.sciencemag.org/cgi/content/full/316/5832/1732/DC1
Materials and Methods
SOM Text
Figs. S1 to S9
Tables S1 to S5
References

31 October 2006; accepted 9 May 2007
10.1126/science.1137004

Saturation of the Southern Ocean CO_2 Sink Due to Recent Climate Change

Corinne Le Quéré,[1,2,3]* Christian Rödenbeck,[1] Erik T. Buitenhuis,[1,2] Thomas J. Conway,[4] Ray Langenfelds,[5] Antony Gomez,[6] Casper Labuschagne,[7] Michel Ramonet,[8] Takakiyo Nakazawa,[9] Nicolas Metzl,[10] Nathan Gillett,[11] Martin Heimann[1]

Based on observed atmospheric carbon dioxide (CO_2) concentration and an inverse method, we estimate that the Southern Ocean sink of CO_2 has weakened between 1981 and 2004 by 0.08 petagrams of carbon per year per decade relative to the trend expected from the large increase in atmospheric CO_2. We attribute this weakening to the observed increase in Southern Ocean winds resulting from human activities, which is projected to continue in the future. Consequences include a reduction of the efficiency of the Southern Ocean sink of CO_2 in the short term (about 25 years) and possibly a higher level of stabilization of atmospheric CO_2 on a multicentury time scale.

Atmospheric CO_2 increases at only half the rate of human-induced CO_2 emissions because of the presence of large CO_2 sinks in the ocean and on land (*1*). The sinks are highly variable and sensitive to climate, yet they are poorly constrained by observations. In the ocean, only the large-scale variability and trends in the equatorial and North Pacific have been quantified (*2*, *3*). In other regions, time-series observations and repeated survey analysis exist, but their extrapolation at the scale of a basin is problematic because of the presence of large regional variability (*4*–*6*). Data are particularly sparse in the Southern Ocean, where the magnitude of the CO_2 sink is heavily disputed (*7*, *8*), its interannual variability is unknown, and its control on atmospheric CO_2 during glaciations is firmly established but still not understood or quantified (*9*, *10*).

We estimated the variability and trend in the CO_2 sink of the Southern Ocean during 1981 to 2004 using the spatiotemporal evolution of atmospheric CO_2 from up to 11 stations in the Southern Ocean and 40 stations worldwide (Fig. 1). We used an inverse method that estimates the CO_2 flux distribution and time variability that best matches the observed atmospheric CO_2 concentrations (*11*). The inversion uses observed atmospheric CO_2 concentrations from individual flask pair values and/or hourly values from in situ analyzers, as available (*12*) (fig. S1). The station set is kept constant throughout the inversion to minimize spurious variability from the inversion setup. We performed an identical inversion over four time periods using (i) 40 atmospheric stations for 1996 to 2004 (9 years), (ii) 25 atmospheric stations for 1991 to 2004 (14 years), (iii) 17 atmospheric stations for 1986 to 2004 time period (19 years), and (iv) 11 atmospheric stations for 1981 to 2004 (24 years). CO_2 fluxes and concentrations are linked by the atmospheric transport model TM3, with resolution of ~4° by 5° and 19 vertical levels, driven by interannual 6-hourly winds from National Centers for Environmental Prediction (NCEP) reanalysis (*13*). The a priori information does not involve any time-dependent elements. Although we focus on the Southern Ocean (south of 45°S), where the influence of the land is at its minimum, the inversion is global.

The variability in integrated sea-air CO_2 flux estimated by the inversions is ±0.14 Pg C $year^{-1}$ (*14*) over the Southern ocean (Fig. 2). The

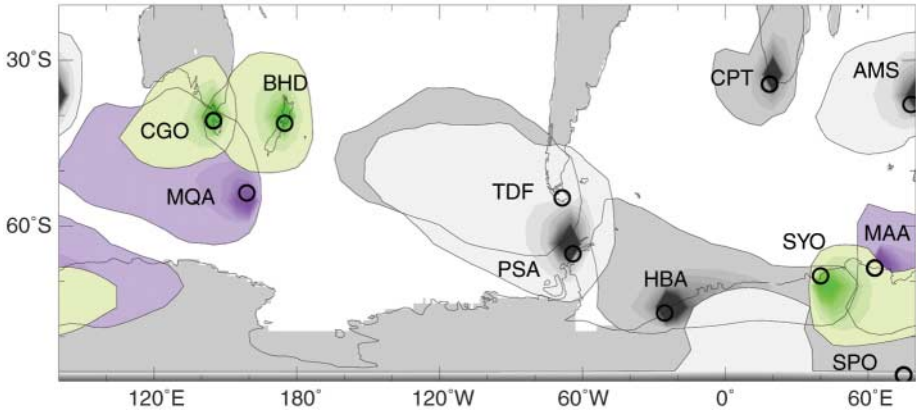

Fig. 1. Footprint of atmospheric CO_2 measurement stations. The footprint is defined here as the area where CO_2 fluxes of 0.2 mol/m^2 $year^{-1}$ produce a concentration response of at least 1 ppm, on an annual average. The darkest shading shows the region with largest influence on a given station. Stations are Cape Grim (CGO; 40.7°S, 144.7°E); Macquarie Island (MQA; 54°S, 159°E); Baring Head (BHD; 41°S, 175°E); Tierra del Fuego (TDF; 54.9°S, 68.5°W); Palmer Station (PSA; 65.0°S, 64°W); Halley Bay (HBA; 75.7°S, 25.5°W); Cape Point (CPT; 34°S, 19°E); Syowa (SYO; 69°S, 39°E); Mawson (MAA; 68°S, 63°E); Amsterdam Island (AMS; 38°S, 78°E); and South Pole (SPO; 90.0°S). The color coding refers to the length of the station's record used, with light gray stations used since 1981, green stations since 1986, purple stations since 1991, and dark gray stations since 1996.

[1]Max Planck Institut für Biogeochemie, Postfach 100164, D-07701 Jena, Germany. [2]School of Environmental Sciences University of East Anglia, Norwich NR4 7TJ, UK. [3]British Antarctic Survey, High Cross, Madingley Road, Cambridge CB3 0ET, UK. [4]National Oceanic and Atmospheric Administration, Earth System Research Laboratory, 325 Broadway, Boulder, CO 80305, USA. [5]Commonwealth Scientific and Industrial Research Organisation, Marine and Atmospheric Research, PMB1 Aspendale, Victoria 3195, Australia. [6]National Institute for Water and Atmospheric Research, P.O. Box 14901, Wellington, New Zealand. [7]South African Weather Service, P.O. Box 320, Stellenbosch, 7599 South Africa. [8]Laboratoire des Sciences du Climat et de l'Environnement/Institut Pierre Simon Laplace (LSCE/IPSL), Gif-sur-Yvettes, Cedex 91191, France. [9]Center for Atmospheric and Oceanic Studies, Tohoku University, Sendai 980-8578, Japan. [10]Laboratoire d'Océanographie et du Climat: Experimentation et Approaches Numériques (LOCEAN/IPSL) CNRS, Université Pierre and Marie Curie, Paris, France. [11]Climate Research Unit, School of Environmental Sciences, University of East Anglia, Norwich NR4 7TJ, UK.

*To whom correspondence should be addressed. E-mail: c.lequere@uea.ac.uk

amplitude of the CO_2 variability is about one-third of the amplitude of the flux variability associated with El Niño events in the equatorial Pacific (*2*) and ~10% of the variability observed in atmospheric CO_2 growth rate (*15*). The longer inversion reproduces most of the variability of the shorter, better constrained inversions.

The longer inversion further shows a decrease of the CO_2 sink in the Southern Ocean between 1981 and 2004 by 0.031 Pg C year^{-1} decade^{-1}. This decrease is significantly different at the 99.5% level (*16*) from the trend of –0.051 Pg C year^{-1} decade^{-1} in sea-air flux expected in response to the increase in atmospheric CO_2 alone (Fig. 2). We estimated the trend caused by increasing atmospheric CO_2 alone using two independent methods. First, we used a simple pulse response function, which we integrated in time using the observed atmospheric CO_2 growth rate as input (top red curve in Fig. 2) (*12*, *17*). This method takes into account the surface ocean equilibration with atmospheric CO_2 and the vertical transport of anthropogenic carbon into the ocean. Second, we used a full Ocean General Circulation Model (OGCM) coupled to a state-of-the-art biogeochemistry model [the Pelagic Interactions Scheme for Carbon and Ecosystem Studies version T (PISCES-T) model; bottom red curve in Fig. 2] (*12*), which we forced with atmospheric surface conditions from either years 1948, 1967, or 1979 repeatedly for all years (three separate simulations, only the 1967 result is plotted in Fig. 2), and with observed atmospheric CO_2 concentration. The pulse response and OGCM estimates have similar variability and a similar trend over the 1981 to 2004 time period (–0.051 and –0.057; –0.046, and –0.072 Pg C year^{-1} decade^{-1}, respectively) (Figs. 2 and 3).

The significant difference between the observed decrease of the CO_2 sink estimated by the inversion (0.03 Pg C year^{-1} decade^{-1}) and the expected increase due solely to rising atmospheric CO_2 (–0.05 Pg C year^{-1} decade^{-1}) indicates that there has been a relative weakening of the Southern Ocean CO_2 sink (0.08 Pg C year^{-1} per decade^{-1}) as a result of changes in other atmospheric forcing (winds, surface air temperature, and water fluxes). For comparison, the mean Southern Ocean CO_2 sink is estimated to be between 0.1 and 0.6 Pg C year^{-1} (table S1).

Inverse methods are sensitive to errors in the setup and transport model, in the data, and in the selection of the sites. We performed three series of sensitivity tests on the inversion results using the longest inversion. In the first series of tests, we assessed the robustness of the results to the choice of the most sensitive parameters of this inversion set up (*11*): (Is1 and Is2) We increased and decreased, respectively, the a priori standard deviation of the ocean and land CO_2 fluxes by a factor of four; (Is3) we increased the a priori standard deviation over the ocean and decreased that over land by a factor of 2 each; (Is4) we increased the spatial correlation scales by a factor of 2 (in latitude) and 4 (in longitude); and (Is5) we decreased the temporal correlation scale by a factor of 4. In the second series of tests, we assessed the robustness of the results with respect to transport errors by degrading the quality of the transport model: (It1) we reduced the resolution of the transport model by a factor of two; and (It2 and It3) we used the degraded model It1 and applied constant winds for years 1990 and 1995, respectively. In the third series of tests, we used the degraded model It1 and included further available data from (Id1) Baring Head, (Id2) Halley Bay, and (Id3) Cape Grim and Syowa, even though they are not available over all the period.

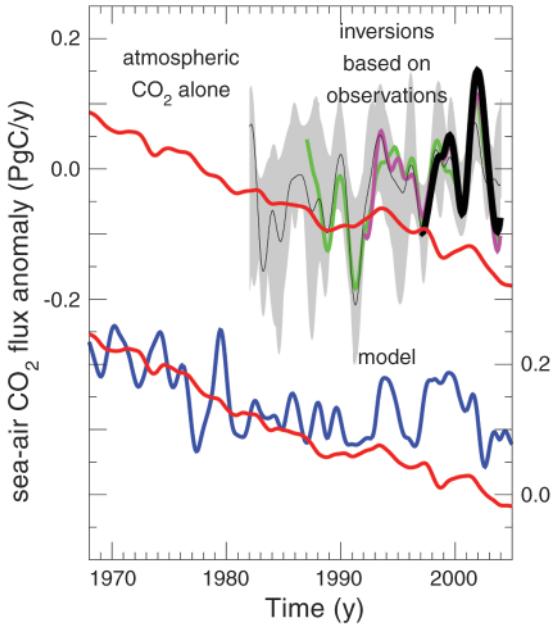

Fig. 2. Sea-air CO_2 flux anomalies in the Southern Ocean (Pg C year^{-1}). The contribution of atmospheric CO_2 alone (top red curve) is calculated based on observed atmospheric CO_2 concentration and a pulse response function that computes the ocean CO_2 uptake as a function of time (*12*, *17*). The estimates based on observations use an inverse model of atmospheric CO_2. Inversions over four time scales are shown starting in 1981 (thin black, 11 sites), 1986 (green, 17 sites), 1991 (purple, 25 sites), and 1996 (thick black, 40 sites). The gray shading encompasses results from all the sensitivity tests using the 11-site inversion. The lower panel shows results from a process model forced by (full red curve) the 1967 constant winds and fluxes and (blue curve) observed daily winds and fluxes from NCEP reanalysis. Sea-air CO_2 fluxes are integrated over 45°S to 90°S. Negative values indicate a flux of CO_2 from the atmosphere to the ocean, or a CO_2 sink into the ocean. Variability <1 year is removed using a Hanning filter for all time series. The 1995 to 2004 average was removed from all inversions (see table S1 for the spread in the mean). The mean of the atmospheric contribution is normalized to the inverted estimate for the 1981 to 1986 time period.

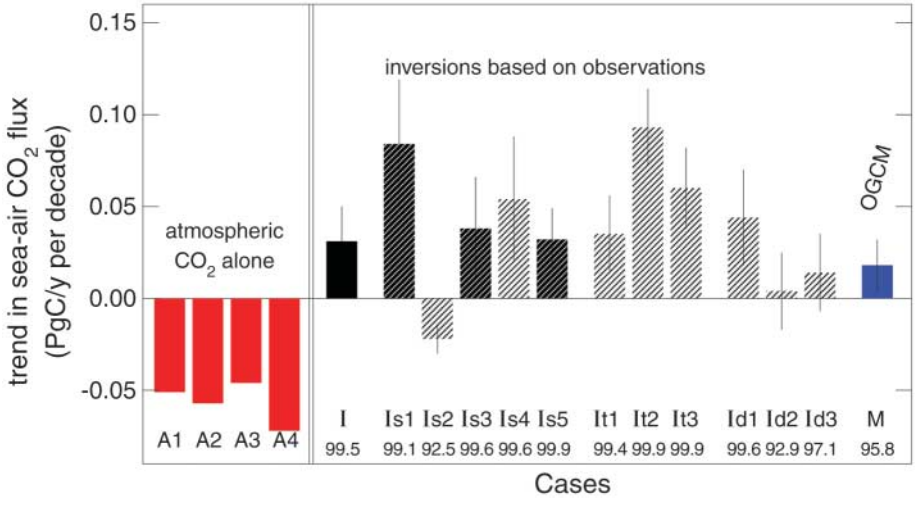

Fig. 3. Trend in the sea-air CO_2 flux (Pg C year^{-1} decade^{-1}). Cases A1 to A4 estimate the contribution of atmospheric CO_2 alone based on a pulse response model (A1) and an OGCM forced by constant winds and atmospheric fluxes (A2 to A4) from years 1948, 1967, and 1979, respectively. All inverse results are shown in black or gray. Case I is the standard inversion. Cases Is1 to Is5 are sensitivity tests to the model parameters. Cases It1 to It3 are sensitivity tests to the atmospheric transport model. Cases Id1 to Id3 are sensitivity tests to the selection of data. The sensitivity tests hatched dark produce the best match to the station data, whereas those hatched light produce the poorest match (*18*). Results of the process model using observed atmospheric forcing are shown in blue (M). Error bars for all cases indicate the amplitude of the interannual variability (± 1 SD). Significance of the departure between all the inversion cases and case A1 and between the model M and case A3 is also shown below each case (*16*).

In all the sensitivity tests, the trend in the CO_2 sink in the Southern Ocean is smaller than the trend caused by increasing atmospheric CO_2 alone (Fig. 3). Inversions I (standard inversion), Is1, Is3, and Is5 produced the best fit to observations (*18*). These inversions showed a decrease in CO_2 sink of 0.03 to 0.08 Pg C year^{-1} decade^{-1}, significantly different at the 99% level from the trend caused by atmospheric CO_2 alone (*16*). The inversions with the degraded transport model fit less well to the station data but still show a decrease in the CO_2 sink significantly different at the 99% level from the expected trend. The only sensitivity test that produces an increase in the CO_2 sink (Is2) also produces the worst fit to the observations (*18*). However, even this inversion produces a smaller increase in the CO_2 sink than that caused by atmospheric CO_2 alone, although the significance level is lower (92.5%).

We assessed the influence of the choice of stations further by comparing the trends in the long inversion with that of the 1986 to 2004 inversion, which uses 17 atmospheric stations instead of 11 (3 additional Southern Ocean stations). The trend in sea-air CO_2 flux in the two inversions for the overlapping period is similar, with 0.047 and 0.035 Pg C year^{-1} decade^{-1} for the 11-station and 17-station inversion, respectively, showing that the trend is correctly captured in the longer inversion.

The CO_2 flux variability from the longest inversion correlates with the Southern Annular Mode (SAM), an index of the dominant mode of atmospheric variability in the Southern Ocean. We use the SAM definition of Marshall (2003) (*19*), based on the difference in mean sea level pressure between 40°S and 65°S, which is entirely based on observations and fully independent of our inversion. The correlation of the monthly mean anomalies is small ($r = +0.22$) but significant at the 99% level (*16*, *18*). The positive correlation indicates that the ocean outgasses CO_2 compared with its mean state when the SAM is positive, i.e., when the winds are intensified south of 45°S (*20*), and suggests that wind-driven upwelling and associated ventilation of the subsurface waters rich in carbon dominates the variability in CO_2 flux (*18*).

To examine whether the results of the inversion can be traced back to physical processes, we estimated the variability and trend in CO_2 fluxes using the OGCM-PISCES-T model (*12*), now forced by daily wind stress and heat and water fluxes from the NCEP reanalyzed data for 1948 to 2004 (*13*), similar to (*21*). This process model reproduces similar patterns of variability in CO_2 flux as estimated by the inversion, with a smaller CO_2 sink (more positive sea-air CO_2 flux) during 1993 to 2003 compared with 1983 to 1993 and 2003 to 2004 (Fig. 2). The process model also produces a decrease in the CO_2 sink between 1981 and 2004 of 0.018 Pg C year^{-1} decade^{-1} (Fig. 3). The difference in sea-air CO_2 trend of +0.064 Pg C year^{-1} decade^{-1} between this simulation using observed atmospheric forcing and the simulation using constant forcing (–0.046 Pg C year^{-1} decade^{-1} using 1967 forcing) is entirely attributable to changes in ocean biogeochemistry caused by changes in surface atmospheric forcing. Thus, the process model attributes the decrease in CO_2 sink to an increase in outgassing of natural carbon (sea-air flux of +0.064 Pg C year^{-1} decade^{-1}) overcompensating the increase in the uptake of anthropogenic CO_2 (sea-air flux of –0.046 Pg C year^{-1} decade^{-1}), in agreement with results of the inversion based on observations.

We performed two additional simulations. First, the winds alone were kept constant at year 1967, but the heat and water fluxes were allowed to vary interannually. Results from this simulation show a trend in sea-air CO_2 flux that is close to the simulation where both winds and fluxes are kept constant (–0.034 compared with –0.046 Pg C year^{-1} decade^{-1}). Second, the winds were kept constant in the formulation of the gas exchange only but were allowed to vary in the physical model. The difference in trend with the variable gas exchange was very small (<3%). The results of the process model suggest that the changes in the CO_2 sink are dominated by the impact of changes in physical mixing and upwelling driven by changes in the winds on the natural carbon cycle in the ocean (*18*) (fig. S5), as suggested by the positive correlation between the inversion and the SAM. The process model also shows that the acidification of the surface ocean is accelerated by this process (*18*) (fig. S5).

On a multicentury time scale, results of simple models based on well-known carbon chemistry show that the ocean should take up 70 to 80% of all the anthropogenic CO_2 emitted to the atmosphere (*22*). This estimate takes into account changes in carbon chemistry but not the physical response of the natural carbon cycle to changes in atmospheric forcing. In the past, the marine carbon cycle has responded to circulation changes and cooling during glaciations by taking up enough carbon to lower atmospheric CO_2 by 80 to 100 parts per million (ppm) (*9*). Changes in Southern Ocean circulation resulting from changes in Southern Ocean winds (*23*) or buoyancy fluxes (*24*) have been identified as the dominant cause of atmospheric CO_2 changes (*9*, *10*, *25*). We showed that the Southern Ocean is responding to changes in winds over a much shorter time scale, thus suggesting that the long-term equilibration of atmospheric CO_2 in the future could occur at a level that is tens of ppm higher than that predicted when considering carbon chemistry alone.

Observations suggest that the trend in the Southern Ocean winds may be a consequence of the depletion of stratospheric ozone (*26*). Models suggest that part of the trend may also be caused by changes in surface temperature gradients resulting from global warming (*27*, *28*). Climate models project a continued intensification in the Southern Ocean winds throughout the 21st century if atmospheric CO_2 continues to increase (*28*). The ocean CO_2 sink will persist as long as atmospheric CO_2 increases, but (i) the fraction of the CO_2 emissions that the ocean is able to absorb may decrease if the observed intensification of the Southern Ocean winds continues in the future and (ii) the level at which atmospheric CO_2 will stabilize on a multicentury time scale may be higher if natural CO_2 is outgassed from the Southern Ocean.

References and Notes

1. I. C. Prentice *et al.*, in *Climate Change 2001: The Scientific Basis. Contribution of Working Group I to the Third Assessment Report of the Intergovernmental Panel on Climate Change*, J. T. Houghton, Y. Ding, D. Griggs, M. Noguer, P. van der Linden, X. Dai, K. Maskell, C. Johnson, Eds. (Cambridge Univ. Press, Cambridge and New York, 2001), pp. 183–237.
2. R. A. Feely, R. Wanninkhof, T. Takahashi, P. Tans, *Nature* **398**, 597 (1999).
3. T. Takahashi, S. C. Sutherland, R. A. Feely, R. Wanninkhof, *Deep-Sea Res.* **111**, 10.1029/2005JC002074 (2006).
4. N. Gruber, C. D. Keeling, N. R. Bates, *Nature* **298**, 2374 (2002).
5. J. E. Dore, R. Lukas, D. W. Sadler, D. M. Karl, *Nature* **424**, 754 (2003).
6. A. Corbière, N. Metzl, G. Reverdin, C. Brunet, T. Takahashi, *Tellus*, doi:10.1111/j.1600-0889.2006.00232.x (2007).
7. T. Roy, P. Rayner, R. Francey, *Tellus* **55B**, 701 (2003).
8. N. Metzl, C. Brunet, A. Jabaud-Jan, A. Poisson, B. Schauer, *Deep-Sea Res. I* **53**, 1548, 10.1016/j.dsr.2006.07.006 (2006).
9. D. M. Sigman, E. Boyle, *Nature* **407**, 859 (2000).
10. K. E. Kohfeld, C. Le Quéré, S. P. Harrison, R. Anderson, *Science* **308**, 74 (2005).
11. C. Rödenbeck, Tech. Rep. 6, Max-Planck-Institute for Biogeochemistry, P.O. Box 100164, 07701 Jena, Germany, 2005. Available on www.bgc-jena.mpg.de/mpg/websiteBiogeochemie/Publikationen/Technical_Reports/tech_report6.pdf.
12. See full description in Supporting Online Material, including a comparison to other published inversions (fig. S2).
13. E. Kalnay *et al.*, *Bull. Am. Meteorol. Soc.* **77**, 437 (1996).
14. 0.28 Pg C year^{-1} for the peak-to-peak monthly anomalies in the longest inversion (1981 to 2004), equivalent to a standard deviation of 0.06 Pg C year^{-1}.
15. C. D. Keeling, T. P. Whorf, in *Trends: A Compendium of Data on Global Change* (Carbon Dioxide Information Analysis Center, Oak Ridge National Laboratory, U.S. Department of Energy, Oak Ridge, TN, 2005).
16. The statistical significance of the trend was estimated using the deseasonalized raw data and a 1000-member Monte Carlo ensemble from a noise model with the same standard deviation and lag-1 autocorrelation (*12*). The statistical significance only assesses the presence of a trend with respect to interannual variability and to random errors in the measurements. The significance of other errors and potential biases caused by the data coverage and inversion setup is assessed by the various sensitivity tests. The trend in the inversion result is not statistically different from zero, but from its expected value based on the increase in atmospheric CO_2 alone.
17. I. G. Enting, T. M. L. Wigley, M. Heimann, *CSIRO Aust. Div. Atmos. Res. Tech. Pap. No.* **31**, 1 (1994).
18. See further model results and evaluation in Supporting Online Material.
19. G. Marshall, *J. Clim.* **16**, 4134 (2003).
20. The increase in zonal winds is best documented by the observed increase in atmospheric pressure gradient between 40°S and 65°S (*19*). The NCEP reanalysis estimates an increase in zonal wind of ~1 to 2 m/s south of 45°S for a mean zonal wind of ~2 to 10 m/s.
21. P. Wetzel, A. Winguth, E. Maier-Reimer, *Global Biogeochem. Cycles* **19**, 10.1029/2004GB002339 (2005).
22. D. E. Archer, H. Kheshgi, E. Maier-Reimer, *Geophys. Res. Lett.* **24**, 405 (1997).
23. R. J. Toggweiler, J. L. Russel, S. Carlson, *Paleoceanogr.* **21**, 10.1029/2005PA001154 (2006).
24. A. J. Watson, A. C. Naveira Garabato, *Tellus* **58B**, 73 (2006).
25. E. W. Wolff *et al.*, *Nature* **440**, 491 (2006).
26. D. W. J. Thompson, S. Solomon, *Science* **296**, 895 (2002).

27. J. Fyfe, G. Boer, G. Flato, *Geophys. Res. Lett.* **26**, 1601 (1999).
28. D. T. Shindell, G. A. Schmidt, *Geophys. Res. Lett.* 10.1029/2004GL020724 (2004).
29. We thank S. Morimoto and everyone who participated in the collection of the atmospheric and oceanic CO_2 observations. The long-term observational project Ocean Indien Service d'Observations (OISO) is conducted on board the research vessel Marion-Dufresne and is supported, like the Amsterdam I. Réseau Atmosphérique de Mesure des Composés à Effet de Serre (RAMCES) observatory, by three Institutes in France, Institut National des Sciences de l'Univers (INSU), Institut Paul Emile Victor (IPEV), and Institut Pierre Simon Laplace (IPSL). We thank N. Gruber, N. Lovenduski, G. Marshall, H. Roscoe, and T. Mitchell for discussions; three anonymous reviewers for insightful comments; K. Rodgers, G. Madec, and the IPSL team for access to model codes; and the Deutsches Klimarechenzentrum (DKRZ) and Gesellschart für wissenschaftliche Datenverarbeitung mbH Göttingen (GWDG) centers for computer support. E.T.B. was partly supported by the EU project CARBOOCEAN (511176[GOCE]) and by the UK NERC/QUEST project Marquest (NE/C516128/1).

Supporting Online Material
www.sciencemag.org/cgi/content/full/1136188/DC1
Methods
Figs. S1 to S8
Tables S1
References

11 October 2006; accepted 2 May 2007
Published online 17 May 2007;
10.1126/science.1136188
Include this information when citing this paper.

Evolutionary Dynamics of Immune-Related Genes and Pathways in Disease-Vector Mosquitoes

Robert M. Waterhouse,[1] Evgenia V. Kriventseva,[2,3] Stephan Meister,[1] Zhiyong Xi,[4] Kanwal S. Alvarez,[5] Lyric C. Bartholomay,[6] Carolina Barillas-Mury,[7] Guowu Bian,[5] Stephanie Blandin,[8] Bruce M. Christensen,[9] Yuemei Dong,[4] Haobo Jiang,[10] Michael R. Kanost,[11] Anastasios C. Koutsos,[1] Elena A. Levashina,[8] Jianyong Li,[12] Petros Ligoxygakis,[13] Robert M. MacCallum,[1] George F. Mayhew,[9] Antonio Mendes,[1] Kristin Michel,[1] Mike A. Osta,[1] Susan Paskewitz,[14] Sang Woon Shin,[5] Dina Vlachou,[1] Lihui Wang,[13] Weiqi Wei,[15,16] Liangbiao Zheng,[15,17] Zhen Zou,[10] David W. Severson,[18] Alexander S. Raikhel,[5] Fotis C. Kafatos,[1]*† George Dimopoulos,[4]* Evgeny M. Zdobnov,[3,19,1]*† George K. Christophides[1]*†

Mosquitoes are vectors of parasitic and viral diseases of immense importance for public health. The acquisition of the genome sequence of the yellow fever and Dengue vector, *Aedes aegypti* (*Aa*), has enabled a comparative phylogenomic analysis of the insect immune repertoire: in *Aa*, the malaria vector *Anopheles gambiae* (*Ag*), and the fruit fly *Drosophila melanogaster* (*Dm*). Analysis of immune signaling pathways and response modules reveals both conservative and rapidly evolving features associated with different functional gene categories and particular aspects of immune reactions. These dynamics reflect in part continuous readjustment between accommodation and rejection of pathogens and suggest how innate immunity may have evolved.

Repeatedly during evolution, mosquitoes and other insects have adopted hematophagy to sustain abundant progeny production. In turn, blood feeding provided a new point of entry for pathogens. To counter assaults, innate immunity has evolved to recognize and respond to numerous pathogens, in a dynamic playoff where either host or pathogen may win. Although fundamental concepts mostly derive from *Dm*, *Ag* is now an important model for studies of innate immunity. A previous comparative analysis of *Ag* and *Dm* immune-related gene families (*1*) highlighted their diversification and pointed toward an expanded conceptual framework of insect innate immunity. The sequencing of the *Aa* genome (*2*) permitted deeper understanding of insect immune systems, as displayed by two quite different mosquito species that diverged ~150 million years ago (Ma) and *Dm*, which separated from them ~250 Ma. This three-way comparison is considerably more powerful than the previous *Dm-Ag* study, because it allows measuring true genetic distances rather than unrooted sequence similarities. Taking advantage of the added value from multiple species comparisons, we explore the evolutionary dynamics of innate immunity in insects and how they can address both common and species-specific immune challenges.

Multiple large-scale bioinformatic methods, manual curation, and phylogenetic analyses (*3*) identified 285 *Dm*, 338 *Ag*, and 353 *Aa* genes from 31 gene families and functional groups implicated in classical innate immunity or defense functions such as apoptosis and response to oxidative stress (table S1). Additional limited analysis of nine sequenced genomes from four holometabolous insect orders, spanning 350 million years of evolution, further defined conserved family features and assisted manual gene model curation by gene family experts. The detailed core analysis (*Aa*/*Ag*/*Dm*) is presented in the supporting online material (SOM) text and in figs. S1 to S22, and the total data set is organized into a web-accessible resource (http://cegg.unige.ch/Insecta/immunodb/), offering a comparative perspective across higher insects. All but 24 previously named *Aa* genes, as well as 79 previously unnamed *Ag* genes, were named in accordance with the nomenclature scheme devised for the *Ag* genome (*1*) with the use of additional guidelines as described in the SOM; this information will be incorporated in the forthcoming manual annotations of the VectorBase resource (www.vectorbase.org).

Our conservative bioinformatic analysis of the complete genomes identified 4951 orthologous trios (1:1:1 orthologs in the three species) and 886 mosquito-specific orthologous pairs (absent from both *Dm* and the honeybee, *Apis mellifera*). Combined bioinformatic analysis and manual curation of the immune repertoire identified 91 trios and 57 pairs, plus a combined total of 589 paralogous genes in the three species. Paralogs derive from family expansions and gene losses, or cases of exceptionally high sequence divergence obscuring phylogenetic relationships. Orthologs most likely serve corresponding functions in respective organisms, whereas paralogs may have acquired different functions.

By definition, orthologous trios represent a numerically conserved subset of genes. Nevertheless, a plot of *Dm-Aa* and *Dm-Ag* phylogenetic distances, measured in terms of amino acid substitutions, revealed that, on average, immunity trio orthologs are significantly more divergent (~20%) than the totality of trios in the genomes

[1]Division of Cell and Molecular Biology, Faculty of Natural Sciences, Imperial College London, London SW7 2AZ, UK. [2]Department of Structural Biology and Bioinformatics, University of Geneva Medical School, 1211 Geneva, Switzerland. [3]Department of Genetic Medicine and Development, University of Geneva Medical School, 1211 Geneva, Switzerland. [4]Department of Molecular Microbiology and Immunology, Bloomberg School of Public Health, Johns Hopkins University, Baltimore, MD 21205, USA. [5]Department of Entomology and the Institute for Integrative Genome Biology, University of California, Riverside, CA 92521, USA. [6]Department of Entomology, Iowa State University, Ames, IA 50011, USA. [7]Laboratory of Malaria and Vector Research, Twinbrook III Facility, National Institute of Allergy and Infectious Diseases (NIAID), National Institutes of Health (NIH), Bethesda, MD 20892–8132, USA. [8]CNRS Unité Propre de Recherche 9022, Avenir-Inserm, Institut de Biologie Moléculaire et Cellulaire, Strasbourg, France. [9]Department of Animal Health and Biomedical Sciences, University of Wisconsin-Madison, Madison, WI 53706, USA. [10]Department of Entomology and Plant Pathology, Oklahoma State University, Stillwater, OK 74078, USA. [11]Department of Biochemistry, Kansas State University, Manhattan, KS 66506, USA. [12]Department of Biochemistry, Virginia Tech, Blacksburg, VA 24061, USA. [13]Department of Biochemistry, University of Oxford, Oxford, UK. [14]Russell Labs, Department of Entomology, University of Wisconsin-Madison, Madison, WI 53706, USA. [15]Yale University School of Medicine, Epidemiology, and Public Health, New Haven, CT 06520, USA. [16]Fujian Center for Prevention and Control of Occupational Disease and Chemical Poisoning, Fujian, China. [17]Institute of Plant Physiology and Ecology, Shanghai, China. [18]Department of Biological Sciences, Center for Global Health and Infectious Diseases, University of Notre Dame, Notre Dame, IN 46556, USA. [19]Swiss Institute of Bioinformatics, 1211 Geneva, Switzerland.

*These authors contributed equally to this work.
†To whom correspondence should be addressed. E-mail: g.christophides@imperial.ac.uk (G.K.C.); zdobnov@medecine.unige.ch (E.M.Z.); f.kafatos@imperial.ac.uk (F.C.K.)

Saturation of the Southern Ocean CO_2 Sink Due to Recent Climate Change

Corinne Le Quéré, Christian Rödenbeck, Erik T. Buitenhuis, Thomas J. Conway, Ray Langenfelds, Antony Gomez, Casper Labuschagne, Michel Ramonet, Takakiyo Nakazawa, Nicolas Metzl, Nathan Gillett and Martin Heimann (May 17, 2007)

Science **316** (5832), 1735-1738. [doi: 10.1126/science.1136188] originally published online May 17, 2007

Editor's Summary